Scientific Research Publishing

Modern Research in Catalysis, 2019, 8, 39-49
https://www.scirp.org/journal/mrc
ISSN Online: 2168-4499
ISSN Print: 2168-4480

Effects of Co_3O_4 Cocatalyst on $InTaO_4$ for Photocatalytic Reduction of CO_2 to CH_3OH under Visible Light Irradiation

Pei-Wen Pan[1], Yu-Wen Chen[1*], Anton S. Brichkov[2], Vladimir V. Kozik[2]

[1]Department of Chemical Engineering, National Central University, Taiwan
[2]Department of Chemistry, Tomsk State University, Tomsk, Russia
Email: *ywchen@cc.ncu.edu.tw

How to cite this paper: Pan, P.-W., Chen, Y.-W., Brichkov, A.S. and Kozik, V.V. (2019) Effects of Co_3O_4 Cocatalyst on $InTaO_4$ for Photocatalytic Reduction of CO_2 to CH_3OH under Visible Light Irradiation. *Modern Research in Catalysis*, **8**, 39-49.
https://doi.org/10.4236/mrc.2019.84004

Received: September 23, 2019
Accepted: October 27, 2019
Published: October 30, 2019

Abstract

$InTaO_4$ was synthesized by a solid-state reaction method using metal oxide as the starting materials. Co was added by incipient-wetness impregnation. The sample was pretreated by H_2 (200 Torr) reduction at 500˚C for 2 h and subsequent O_2 (100 Torr) oxidation at 200˚C for 1 h. The core-shell structure of metallic Co and Co_3O_4 was formed by this reduction-oxidation procedure. The catalysts were characterized by powder X-ray diffraction, scanning electron microscope, and ultraviolet-visible spectroscope. The photocatalytic reduction was carried out in a Pyrex reactor with $KHCO_3$ or NaOH aqueous solution bubbled with ultra pure CO_2 gas under visible light illumination. SEM micrographs show many small Co_3O_4 particles on the surface of $InTaO_4$. The band gap of Co_3O_4-$InTaO_4$ was 2.7 eV, confirming that these catalysts have the ability to reduce CO_2 to methanol. The methanol yield increased with the amount of Co_3O_4 cocatalysts. The catalyst had a higher activity in $KHCO_3$ aqueous solution than in NaOH solution. The $InTaO_4$ catalyst with 1 wt% Co_3O_4 cocatalyst had the highest activity among all catalysts. Co_3O_4 was incorporate into the surface structure of $InTaO_4$ to form Co_xInTaO_{4-x}. It resulted in more defect sites on the surface of $InTaO_4$ and changed the valence band structure. It formed a Schottky barrier to suppress the electron-hole recombination.

Keywords

Carbon Dioxide, Utilization, Photoreduction, Methanol Formation, Visible Light Irradiation

1. Introduction

Photocatalytic reduction of carbon dioxide to methane and methanol has been

extensively studied by many researchers [1]-[6]. Anpo *et al.* [7] carried out a series of research on Ti-zeolite and Ti-mesoporous materials since 1997. Several photocatalysts were reported, such as Ti-oxide/Y-zeolite [8], Ti-MCM-41 [9], Ti-MCM-48 [9], FSM-16 [10] [11], Ti-β zeolite [12], and self-standing porous silica thin films [13] [14] [15], etc. It is important to use the catalysts with low energy band gap, because the lower the band gap is, the easier the photon excited [16] [17] [18] [19].

$InMO_4$ (M = Ta, Nb, V) catalysts have been reported as photoactive for water splitting reaction under visible light [20] [21] [22] [23]. According to the band structures of $InTaO_4$, the photoreduction of carbon dioxide on $InTaO_4$ catalysts should be feasible. Our previous study [24] showed that NiO-$InTaO_4$ was active for photoreduction of CO_2 to produce methanol. It has been reported that other cocatalysts such as Co_3O_4 [25] [26] are effective. However, it has not been reported in literature for photoreduction of CO_2 [27] [28] [29].

In this study, the Co_3O_4-$InTaO_4$ with various Co_3O_4 contents was synthesized. The catalysts were characterized by powder X-ray diffraction, scanning electron microscope, and ultraviolet-visible spectroscopy. The photocatalytic activities of Co_3O_4-$InTaO_4$ photocatalysts for CO_2 reduction under visible light irradiation were investigated.

2. Experimental

2.1. Catalyst Preparation

The polycrystalline $InTaO_4$ was synthesized by a solid-state reaction method as reported in literature [24]. The pre-dried In_2O_3 and Ta_2O_5 were used as the starting materials. The stoichiometric amounts of precursors were mixed and reacted in an aluminum crucible in air at 1100˚C for 12 h. The material was stirred at least 3 times during preparation to ensure well mix of starting materials.

Co_3O_4-$InTaO_4$ samples with various Co_3O_4 cocatalyst (0.3 wt%, 0.5 wt% and 1 wt%, respectively) were prepared by incipient-wetness impregnation with aqueous solution of $Co(NO_3)_2$. After preparation, the sample was heated by a water bath at 100˚C. The dried powder was then calcined at 400˚C for 4 h in an oven. The sample was pretreated by H_2 (200 Torr) reduction at 500˚C for 2 h and subsequent O_2 (100 Torr) oxidation at 200˚C for 1 h. The core-shell structure of metallic Co and Co_3O_4 was formed by this reduction-oxidation procedure.

2.2. Catalyst Characterization

2.2.1 X-Ray Diffraction (XRD)

The XRD experiments were performed using a Siemens D-500 powder diffractometer with Cu-K_α radiation (40 kV, 41 mA), 0.024˚ step size and 1 sec step time from 5˚ to 90˚. The detailed experimental procedure has been reported in the previous literature [25]. The Bragg-Brentano focusing geometry was em-

ployed with an automatic divergence slit (irradiated sample length was 12.5 nm), a receiving slit of 0.1 nm, a fixed slit of 4˚ and a proportional counter as a detector.

2.2.2. Scanning Electron Microscopy (SEM)

The detailed experimental procedure has been reported in previous literature [25]. Briefly, the samples were placed on an aluminum stage specially made for SEM. The samples were sputter-coated with Au for 90 s before the experiment began. The microstructure and morphology of the materials were examined using a scanning electron microscope (Hitachi S-800) with a field gun. An accelerating voltage of 20 kV was used. The composition of the samples was determined by X-ray energy dispersion spectrum (EDS) with accelerating voltage of 20 kV.

2.2.3. Ultraviolet-Visible Spectroscopy (UV-vis)

The diffuse reflectance UV-vis was measured with a Cary 300 Bio UV-visible Spectrophotometer. Powder samples were loaded in a quartz cell with Suprasil windows, and the spectra were collected in the range from 300 nm to 800 nm against quartz standard.

2.3. Photocatalytic Reaction

Photocatalytic reactions were carried out in a continuous flow reactor. The detailed reaction procedure was described in previous literature [25]. The catalyst powder (0.14 g) was dispersed in a reactant solution (50 mL) in a down-window type irradiation cell made of Pyrex glass (75 ml). 0.2 M Sodium hydroxide aqueous solution or 0.2 M potassium bicarbonate aqueous solutions were employed as an absorbent of carbon dioxide and the ultra pure CO_2 were added continuously into the reactor for 1 h to remove the oxygen in the water, and saturated carbon dioxide in the solution. Using the cooling system combined with water pump, the temperature of the reactor was maintained at room temperature. Light on to start the reaction, and the irradiation was continued for 20 h. The light source was a 500 W halogen lamp (Ever bright; H-500). After reaction for 20 h, the reaction solution was centrifuged for 10 min to separate the reaction products from the powder catalyst. 10 mL of the upper stratum was taken for analyzing the concentration of methanol. The amount of methanol was determined by a gas chromatography equipped with a flame ionization detector, using Poropack-QS column.

3. Results and Discussion

3.1. XRD

Figure 1 shows the XRD patterns of the Co_3O_4-$InTaO_4$ samples. The XRD patterns of $InTaO_4$ samples are well consistent with monoclinic $InTaO_4$ pattern and space group P2/c, indicating that the samples were fully crystallized in the wolframite-type structure. $InTaO_4$ has major peaks at around $2\theta = 23.967^\circ$ (−110),

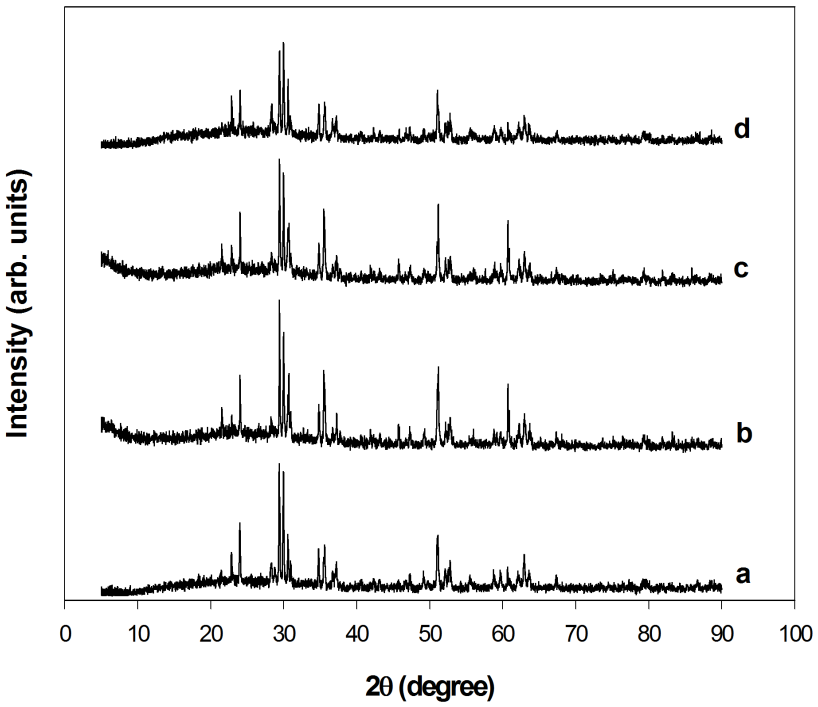

Figure 1. XRD patterns of $InTaO_4$ with various amounts of Co_3O_4 cocatalysts. (a) $InTaO_4$, (b) 0.3 wt%, (c) 0.5 wt% and (d) 1.0 wt% Co_3O_4-$InTaO_4$.

29.356˚ (−111) and 29.899˚ (111) [20] [21] [22] [23] [24]. The lattice parameters of the crystal were refined as: a = 4.83300 (−1) Å, b = 5.77800 (1) Å, c = 5.15700 (1) Å and β = 91.380˚. The indexed results are in good agreement with those reported in the JCPDS database card (No. 25-0391). Zou and his coworkers [20] have reported the structural refinements of $InTaO_4$. The $InTaO_4$ compound belongs to a monoclinic system with space group P2/c, a = 5.1552 (1), b = 5.7751 (1), c = 4.8264 (1) Å and β = 91.373 (1)˚. The structure is composed of two kinds of octahedral: InO_6 octahedron and TaO_6 octahedron. The InO_6 octahedron connects to each other to form zigzag chains by sharing edge. These InO_6 chains are connected through TaO_6 octahedron to form the three dimensional network.

Figure 1 also shows that the characteristic XRD peaks corresponding to Co species such as Co_3O_4 were not observed in the XRD patterns, indicating that the Co species on $InTaO_4$ was too small to detect. There was no difference in XRD patterns between $InTaO_4$ and 1.0 wt% Co_3O_4-$InTaO_4$, indicating that the addition of Co_3O_4 cocatalyst on the surface of $InTaO_4$ did not change the bulk structure of $InTaO_4$. However, it could modify the surface of $InTaO_4$ as discussed in the latter section. One can conclude that Co_3O_4 nanoparticles were well dispersed on the surface of $InTaO_4$.

3.2. SEM

Figure 2 shows the SEM photographs of $InTaO_4$ samples with various amounts of Co_3O_4 cocatalysts. The particle size of $InTaO_4$ was about 0.5 μm. Many nano Co_3O_4 particles were present on $InTaO_4$ surface, in consistent with XRD results.

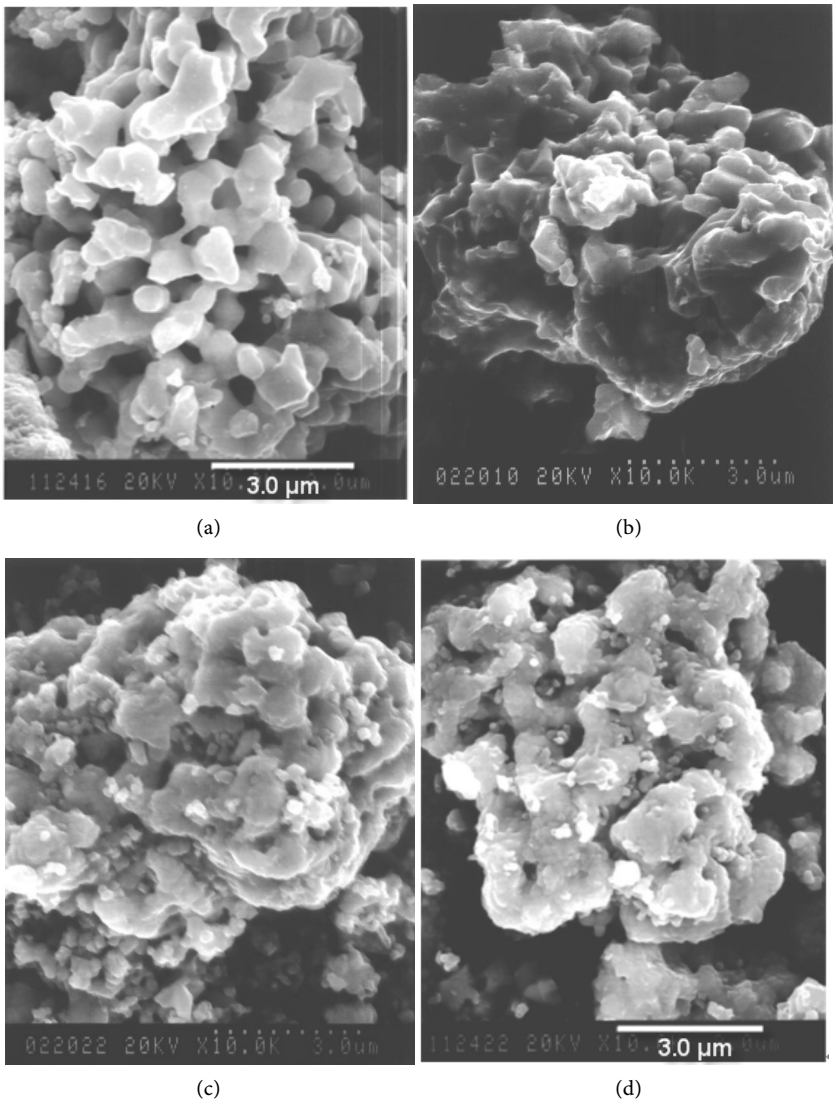

(a) (b)

(c) (d)

Figure 2. SEM micrographs, (a) $InTaO_4$, (b) 0.3 wt% Co_3O_4-$InTaO_4$, (c) 0.5 wt% Co_3O_4-$InTaO_4$, and (d) 1.0 wt% Co_3O_4-$InTaO_4$.

3.3. UV-vis Spectroscopy

Photocatalytic activity is dependent on the band structure of semiconductor. The information of band structure is very important for understanding photocatalytic reaction. **Figure 3** shows the diffuse reflectance spectra of $InTaO_4$ samples with various amounts of Co_3O_4 loading. It shows higher light absorption ability of Co_3O_4/$InTaO_4$ in the visible light compared with $InTaO_4$. The band gap of $InTaO_4$ was 3.0 eV. For 0.3, 0.5, and 1.0 wt% Co_3O_4-$InTaO_4$ catalysts after calcinations, an obvious absorption in the visible light region were observed on all catalysts. The absorbance of the sample increased with increasing the amount of Co_3O_4 cocatalysts. The band gap of 0.3, 0.5, and 1.0 wt% Co_3O_4-$InTaO_4$ were calculated to be 2.8 eV, 2.7 eV and 2.6 eV, respectively (**Table 1**). The results indicate that adding Co_3O_4 cocatalyst on $InTaO_4$ changed the band gap. The bangap of the catalyst decreased with an increase of Co_3O_4 loading.

Table 1. Band gap of Co_3O_4-$InTaO_4$.

Photocatalysts	E_g (eV)
$InTaO_4$	3.0
0.3 wt% Co_3O_4-$InTaO_4$	2.8
0.5 wt% Co_3O_4-$InTaO_4$	2.7
1.0 wt% Co_3O_4-$InTaO_4$	2.6

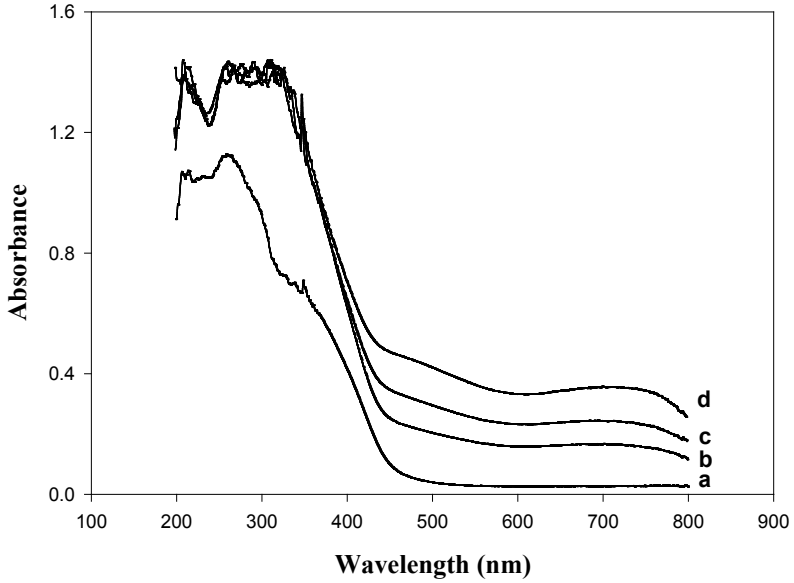

Figure 3. UV-vis spectra, (a) $InTaO_4$, (b) 0.3 wt% Co_3O_4-$InTaO_4$, (c) 0.5 wt% Co_3O_4-$InTaO_4$, and (d) 1.0 wt% Co_3O_4-$InTaO_4$.

3.4. Photocatalytic Reaction

The activities of carbon dioxide reduction on $InTaO_4$ samples with various Co_3O_4 loadings are shown in **Figure 4**. All catalysts produced methanol from the photoreduction of CO_2 under visible light irradiation. No other products were detected in gas phase and liquid phase. The rate of the reaction product increased linearly with the visible light-irradiation time, and the reaction stopped immediately when the irradiation was ceased. The formation of the reaction product was not detected under dark conditions. The reaction rate varied with the smount of cocatalyst. The results in **Figure 4** were obtained from the $InTaO_4$ catalyst with Co_3O_4 cocatalyst suspended in 0.2 M NaOH and 0.2 M $KHCO_3$ aqueous solution. The highest methanol yield of 1.0 wt% Co_3O_4-$InTaO_4$ was 1.150 μmol.h^{-1} g catal.$^{-1}$. In the NaOH solution, 0.5 wt% Co_3O_4-$InTaO_4$ demonstrated the highest methanol yield, and the Co_3O_4 cocatalyst enhanced the production of methanol. The Co_3O_4 cocatalyst not only provides reaction centers, which effectively transfer the electrons from the surface of catalysts to Co, but also enhances the light absorbance.

The results showed that the photocatalytic reduction was induced by the visible light irradiation. The formation rate of methanol increased with the presence

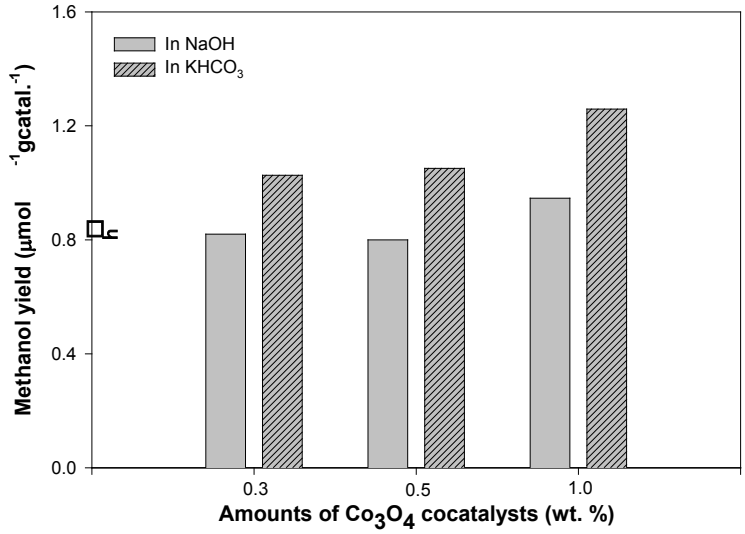

Figure 4. Methanol yield of photoreduction of CO_2 on $InTaO_4$ with various amounts of Co_3O_4 cocatalysts after pretreatment in 0.2 M NaOH and 0.2 M $KHCO_3$ aqueous solutions, under visible light irradiation. Catalyst: 0.14 g; Volume of the solution: 50 ml.

of cocatalysts on $InTaO_4$ photocatalysts. The photocatalyst had a higher activity in $KHCO_3$ aqueous solution than in NaOH solution, in agreement with literature results [17]. The $InTaO_4$ catalyst with 1.0 wt% Co_3O_4 cocatalyst in $KHCO_3$ aqueous solution gave the highest yield of methanol among all catalysts.

In the case of 1.0 wt% Co_3O_4-$InTaO_4$, Co_3O_4 species were loaded on $InTaO_4$ as nanoparticles, which were not observed by SEM analysis. However, after pretreatment, there was a formation of bulky Co_3O_4 particles on $InTaO_4$ due to aggregation of Co_3O_4 nanoparticles, leading to low photocatalytic activity. Bulk Co_3O_4 is a p-type semiconductor, which induces the formation of positive holes. For photoreduction of CO_2, hole scavengers are necessary to facilitate photoreduction; consequently, bulk Co_3O_4 reduced the photocatalytic activity of 1.0 wt% Co_3O_4–$InTaO_4$ catalyst. Hence, it is necessary to avoid the formation of bulk Co_3O_4.

The characterization results of 0.5 wt% Co_3O_4-loaded $InTaO_4$ photocatalyst showed the presence of ultra-fine Co_3O_4 thin films on metallic cobalt particles. The high dispersion of Co_3O_4 particles on the surface and interface of $InTaO_4$ plays a major role in determining its photocatalytic activity. The metallic cobalt acts as a bias for electron transfer from $InTaO_4$ to Co_3O_4 layer and the excited electron can migrate easily to the surface to facilitate photoreduction of CO_2. Methanol acts as a hole scavenger to improve the yield.

It should be noted that for dry $InTaO_4$, all the donor states are occupied and no optical transitions from the valence band to the donor state occurs. Instead, when $InTaO_4$ is immersed in water, partial depletion of the donor states will occur. This leads to band bending and the formation of a depletion layer, as reported in literature [23] [27] [28] [29]. The ionized donor states can be filled through optical excitation of valence band electrons, which explains the sub-bandgap optical absorption of $InTaO_4$ and high photoactivity of $InTaO_4$ in

liquid phase reduction of CO_2. Zou *et al.* [20] reported that the bottom of conduction band of Ta_{3d} is lower than conduction band level of Co_3O_4. Accordingly, the conduction band level of the $Co_3O_4/InTaO_4$ is not high enough for electrons transfer across $InTaO_4$ and Co_3O_4 interface. Co cations are presumably located on the Ta^{3+} sites, especially when one considers that the formation of singly charged acceptor defects is energetically much more favorable than the formation of the triply charged defects that would be formed if any Co would substitute for Ta^{5+}. Since Co_3O_4 was added after formation of full crystallite of $InTa_4$. Co_3O_4 did not incorporate into bulk $InTaO_4$ crystal. Co_3O_4 was incorporate into the surface structure of $InTaO_4$ as Co_xInTaO_{4-x}. It resulted in more defect sites on the surface of $InTaO_4$ and changed the valence band structure and the surface became a Schottky barrier to suppress the recombination of electron and holes. The higher light absorption ability of $Co_3O_4/InTaO_4$ in the visible light compared with $InTaO_4$ was also responsible for the high activity of $Co_3O_4/inTaO_4$ catalysts.

4. Conclusion

$InTaO_4$ was synthesized by a solid-state reaction method using metal oxide as the starting materials. Various amounts of Co were added by incipient-wetness impregnation method. The catalysts were characterized by powder X-ray diffraction, scanning electron microscope, and ultraviolet-visible spectroscope. The photocatalytic reduction was carried out in a Pyrex reactor with $KHCO_3$ or NaOH aqueous solution bubbled with CO_2 gas under visible light illumination. SEM micrographs show the appearance of many small Co_3O_4 particles on $InTaO_4$. The band gap of Co_3O_4-$InTaO_4$ was 2.7 eV, showing that these catalysts have the ability to reduce CO_2 to methanol. The effect of adding various amounts of cocatalysts on the photocatalytic reduction was investigated. The methanol yield increased with the amount of Co_3O_4 cocatalyst. The photocatalyst had a higher activity in $KHCO_3$ aqueous solution than in NaOH aqueous solution. The reaction on $InTaO_4$ catalyst with 1.0 wt% Co_3O_4 cocatalyst had the highest yield of methanol among all catalysts. Co_3O_4 was incorporate into the surface structure of $InTaO_4$ as Co_xInTaO_{4-x}. It resulted in more defect sites on the surface of $InTaO_4$ and changed the valence band structure. The surface became a Schottky barrier to suppress the recombination of electron and holes. The higher light absorption ability of $Co_3O_4/InTaO_4$ in the visible light compared with $InTaO_4$ was also responsible for the high activity of $Co_3O_4/inTaO_4$ catalysts.

Acknowledgements

This research was supported by Ministry of Science and Technology, Taiwan.

Conflicts of Interest

The authors declare no conflicts of interest regarding the publication of this paper.

References

[1] Li, K., An, X., Park, K.H., Khraisheh, M. and Tang, J. (2014) A Critical Review of CO_2 Photoconversion: Catalysts and Reactors. *Catalysis Today*, **224**, 3-15. https://doi.org/10.1016/j.cattod.2013.12.006

[2] Guan, G., Kida, T., Harada, T., Isayama, M. and Yoshida, A. (2003) Photoreduction of Carbon Dioxide with Water over $K_2Ti_6O_{13}$ Photocatalyst Combined with Cu/ZnO Catalyst under Concentrated Sunlight. *Applied Catalysis B: Environmental*, **41**, 387-394. https://doi.org/10.1016/S0926-860X(03)00205-9

[3] Neațu, Ș., Maciá-Agulló, J.A. and Garcia, H. (2014) Solar Light Photocatalytic CO_2 Reduction: General Considerations and Selected Bench-Mark Photocatalysts. *International Journal of Molecular Sciences*, **15**, 5246-5524. https://doi.org/10.3390/ijms15045246

[4] Anpo, M. and Kamat, P.V. (2010) Environmentally Benign Photocatalysts, Applications of Titanium Oxide-Based Materials. Springer, New York. https://doi.org/10.1007/978-0-387-48444-0

[5] Schneider, J., Matsuoka, M., Takeuchi, M., Zhang, J., Horiuchi, Y., Anpo, M. and Bahnemann, D.W. (2014) Understanding TiO_2 Photocatalysis: Mechanisms and Materials. *Chemical Reviews*, **114**, 9919-9925. https://doi.org/10.1021/cr5001892

[6] Anpo, M. (2013) Photocatalytic Reduction of CO_2 with H_2O on Highly Dispersed Ti-Oxide Catalysts as a Model of Artificial Photosynthesis. *Journal of CO_2 Utilization*, **1**, 8-20. https://doi.org/10.1016/j.jcou.2013.03.005

[7] Anpo, M., Yamashita, H., Ichihashi, Y., Fujii, Y. and Honda, M. (1997) Photocatalytic Reduction of CO_2 with H_2O on Titaniun Oxide Anchored within Micropores of Zeolite: Effect of the Structure of the Active Sites and the Addition of Pt. *The Journal of Physical Chemistry B*, **101**, 2632-2636. https://doi.org/10.1021/jp962696h

[8] Anpo, M., Takeuchi, M., Ikeue, K. and Dohshi, S. (2002) Design and Development of Titanium Oxide Photocatalysts Operating under Visible and UV Light Irradiation. The Application of Metal Ion-Implantation Techniques to Semiconducting TiO_2 and Ti/Zeolite Catalysts. *Current Opinion in Solid State & Materials Science*, **6**, 381-388. https://doi.org/10.1016/S1359-0286(02)00107-9

[9] Anpo, M., Yamashita, H., Ikeue, K., Fujii, Y., Zhang, S.G., Ichihashi, Y., Park, D.R., Suzuki, Y., Koyano, K. and Tatsumi, T. (1998) Photocatalytic Reduction of CO_2 with H_2O on Ti-MCM-41 and Ti-MCM-48 Mesoporous Zeolite Catalysts. *Catalysis Today*, **44**, 327-334. https://doi.org/10.1016/S0920-5861(98)00206-5

[10] Ikeue, K., Mukai, H., Yamashita, H., Inagaki, S., Matsuoka, M. and Anpo, M. (2001) Characterization and Photocatalytic Reduction of CO_2 with H_2O on Ti/FSM-16 Synthesized by Various Preparation Methods. *Journal of Synchrotron Radiation*, **8**, 640-646. https://doi.org/10.1107/S0909049500013674

[11] Ikeue, K., Yamashita, H. and Anpo, M. (1999) Photocatalytic Reduction of CO_2 with H_2O on Titanium Oxide Prepared within the FSM-16 Mesoporous Zeolite. *Chemistry Letters*, **28**, 1135-1139. https://doi.org/10.1246/cl.1999.1135

[12] Ikeue, K., Yamashita, H. and Anpo, M. (2001) Photocatalytic Reduction of CO_2 with H_2O on Ti-β Zeolite Photocatalysts: Effect of the Hydrophobic and Hydrophilic Properties. *The Journal of Physical Chemistry B*, **105**, 8350-8358. https://doi.org/10.1021/jp010885g

[13] Ikeue, K., Nozaki, S., Ogawa, M. and Anpo, M. (2002) Characterization of Self-Standing Ti-Containing Porous Silica Thin Film and Their Reactivity for the Photocatalytic Reduction of CO_2 with H_2O. *Catalysis Today*, **74**, 241-246. https://doi.org/10.1016/S0920-5861(02)00027-5

[14] Ikeue, K., Nozaki, S., Ogawa, M. and Anpo, M. (2002) Photocatalytic Reduction of CO_2 with H_2O on Ti-Containing Porous Silica Thin Film Photocatalysts. *Catalysis Letters*, **80**, 111-116.

[15] Shioya, Y., Ikeue, K., Ogawa, M. and Anpo, M. (2003) Synthesis of Transparent Ti-Containing Mesoporous Silica Thin Film Materials and Their Unique Photocatalytic Activity for the Reduction of CO_2 with H_2O. *Applied Catalysis A*: *General*, **254**, 251-258. https://doi.org/10.1016/S0926-860X(03)00487-3

[16] Yamashita, H., Fujii, Y., Ichihashi, Y., Zhang, S.G., Ikeue, K., Park, D.R., Koyano, K., Tatsumi, T. and Anpo, M. (1998) Selective Formation of CH_3OH in the Photocatalytic Reduction of CO_2 with H_2O on Titantium Oxide Highly Dispersed within Zeolites and Mesoporous Molecular Sieves. *Catalysis Today*, **45**, 221-227. https://doi.org/10.1016/S0920-5861(98)00219-3

[17] Ku, Y., Lee, W.H. and Wang, W.Y. (2004) Photocatalytic Reduction of Carbonate in Aqueous Solution by UV/TiO_2 Process. *Journal of Molecular Catalysis A*: *Chemical*, **212**, 191-198. https://doi.org/10.1016/j.molcata.2003.10.047

[18] Matsuoka, M. and Anpo, M. (2003) Review, Local Structures, Excited States, and Photocatalytic Reactivities of Highly Dispersed Catalysts Constructed within Zeolites. *Journal of Photochemistry and Photobiology C*: *Photochemistry Reviews*, **3**, 225-240. https://doi.org/10.1016/S1389-5567(02)00040-0

[19] Inoue, T., Fujishima, A., Konishi, S. and Honda, K. (1979) Photoelectrocatalytic Reduction of Carbon Dioxide in Aqueous Suspensions of Semiconductor Powders. *Nature*, **277**, 637-644. https://doi.org/10.1038/277637a0

[20] Zou, Z., Ye, J. and Arakawa, K. (2000) Structural Properties of $InNbO_4$ and $InTaO_4$: Correlation with Photocatalytic and Photophysical Properties. *Chemical Physics Letters*, **332**, 271-277. https://doi.org/10.1016/S0009-2614(00)01265-3

[21] Matsushima, S., Obata, K., Nakamura, H., Arai, M. and Kobayashi, K. (2003) First-Principles Energy Band Calculation for Undoped and N-Doped $InTaO_4$ with Layered Wolframite-Type Structure. *Journal of Physics and Chemistry of Solids*, **64**, 2417-2421. https://doi.org/10.1016/S0022-3697(03)00283-X

[22] Zeng, G.S., Yu, J., Zhu, H.Y., Liu, H.L., Xing, Q.J., Bao, S.K., He, S., Zou, J.P. and Au, C.T. (2015) Controllable Synthesis of $InTaO_4$ Catalysts of Different Morphologies Using a Versatile Sol Precursor for Photocatalytic Evolution of H_2. *RSC Advances*, **5**, 37603-37609. https://doi.org/10.1039/C5RA03638K

[23] Singhal, N., Goyal, R. and Kumar, U. (2017) Visible-Light-Assisted Photocatalytic CO_2 Reduction over $InTaO_4$: Selective Methanol Formation. *Energy Fuels*, **31**, 12434-12438. https://doi.org/10.1021/acs.energyfuels.7b02123

[24] Pan, P.W. and Chen, Y.W. (2007) Photocatalytic Reduction of Carbon Dioxide on NiO/$InTaO_4$ under Visible Light Irradiation. *Catalysis Communications*, **8**, 1546-1549. https://doi.org/10.1016/j.catcom.2007.01.006

[25] Lee, D.S. and Chen, Y.W. (2015) Photocatalytic Reduction of Carbon Dioxide with Water on $InVO_4$ with NiO Cocatalysts. *Journal of CO_2 Utilization*, **10**, 1-6. https://doi.org/10.1016/j.jcou.2015.02.005

[26] Lee, D.S., Chen, H.J. and Chen, Y.W. (2012) Photcatalytic Reduction of Carbon Dioxide with Water using $InNbO_4$ Catalyst with NiO and Co_3O_4 Cocatalysts. *Journal of Physics and Chemistry of Solids*, **73**, 661-667. https://doi.org/10.1016/j.jpcs.2012.01.005

[27] Malingowski, A.C., Stephens, P.W., Huq, A., Huang, Q., Khalid, S. and Khalifah, P.G. (2012) Substitutional Mechanism of Ni into the Wide-Band-Gap Semiconductor $InTaO_4$ and Its Implications for Water Splitting Activity in the Wolframite

Structure Type. *Inorganic Chemistry*, **111**, 6096-6103. https://doi.org/10.1021/ic202715c

[28] Botella, P., Errandonea, D. and Garg, A.B. (2019) High-Pressure Characterization of the Optical and Electronic Properties of $InVO_4$, $InNbO_4$, and $InTaO_4$. *Applied Sciences*, **1**, 389-396. https://doi.org/10.1007/s42452-019-0406-7

[29] Scaife, D.E. (1980) Oxide Semiconductors in Photoelectrochemical Conversion of Solar Energy. *Solar Energy*, **25**, 42-54. https://doi.org/10.1016/0038-092X(80)90405-3